

# Development of a Photoelectric Adjustment System With Extended Range for Fluorescence Immunoassay Strip Readers

Volume 13, Number 3, June 2021

Huihuang Wu

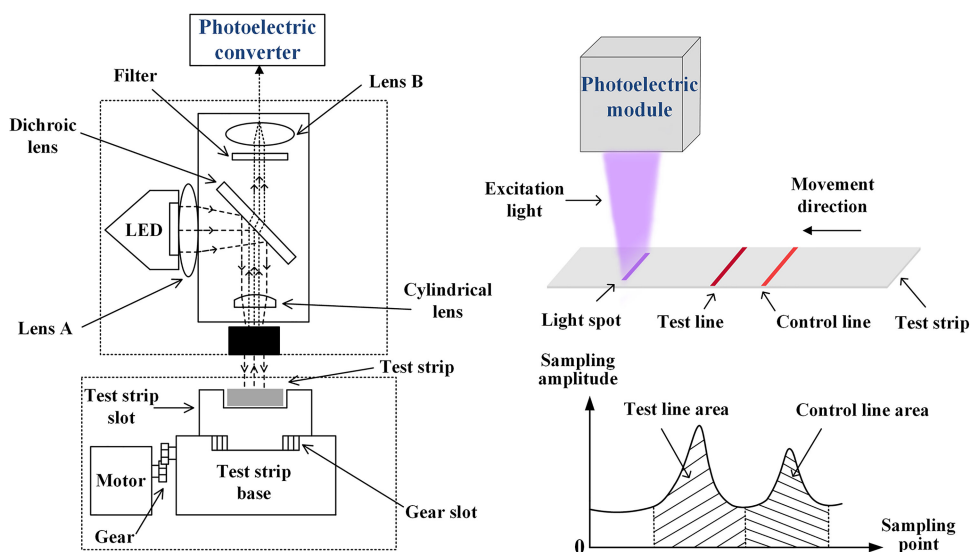
Yueming Gao, *Member, IEEE*

Jiejie Yang

Mangi Vai, *Senior Member, IEEE*

Min Du

Siohang Pun, *Senior Member, IEEE*



DOI: 10.1109/JPHOT.2021.3075900

# Development of a Photoelectric Adjustment System With Extended Range for Fluorescence Immuno-chromatographic Assay Strip Readers

Huihuang Wu <sup>1,2</sup>, Yueming Gao <sup>1,2</sup> *Member, IEEE*, Jiejie Yang,<sup>1,2</sup>  
Mangi Vai,<sup>2,4,5</sup> *Senior Member, IEEE*, Min Du,<sup>1,3</sup>  
and Sihang Pun,<sup>4</sup> *Senior Member, IEEE*

<sup>1</sup>College of Physics and Information Engineering, Fuzhou University, Fuzhou 350108, China

<sup>2</sup>Key Lab of Medical Instrumentation & Pharmaceutical Technology of Fujian Province, Fuzhou 350108, China

<sup>3</sup>Key Lab of Eco-Industrial Green Technology of Fujian Province, Nanping 354300, China

<sup>4</sup>State Key Laboratory of Analog and Mixed-Signal VLSI, University of Macau, Macau 999078, Macau SAR, China

<sup>5</sup>Department of Electrical and Computer Engineering, Faculty of Science and Technology, University of Macau, Macao 999078, China

DOI:10.1109/JPHOT.2021.3075900

This work is licensed under a Creative Commons Attribution-NonCommercial-NoDerivatives 4.0 License. For more information, see <https://creativecommons.org/licenses/by-nc-nd/4.0/>

Manuscript received December 28, 2020; revised April 20, 2021; accepted April 22, 2021. Date of publication April 27, 2021; date of current version May 20, 2021. This work was supported in part by the Project of Chinese Ministry of Science and Technology under Grant 2012DFM30040, in part by the National Natural Science Foundation of China under Grant U1505251, and in part by the Project of Fujian Provincial Department of Science and Technology under Grant 2014YZ0001. Corresponding author: Yueming Gao (e-mail: fzugym@163.com).

**Abstract:** Fluorescence immuno-chromatographic assay (FICA) is a quantitative detection technique widely used in clinical diagnosis, environmental monitoring, and food safety. To deal with the limited applications caused by insufficient detection range, this paper proposes a photoelectric adjustment system suitable for FICA strip readers to expand its detection range. The photoelectric adjustment system is proposed based on the relationship between the excitation light intensity and the fluorescence intensity, which provides the optimal excitation light intensity and a stable baseline amplitude for the FICA strip reader. To verify the proposed system, it was applied to the strip reader we had previously developed. The results show that the linear detection range of the FICA strip reader was extended from 1.95-256  $\mu\text{g/mL}$  to 1-1024  $\mu\text{g/mL}$  after using the proposed method. At the same time, the accuracy of the FICA strip reader does not deteriorate and is in good comparisons with the conventional ESEQuant Lateral Flow Reader (with  $R^2 > 0.9987$ ). Therefore, the proposed photoelectric adjustment method and system can improve the detection range of the strip reader or other similar devices.

**Index Terms:** Fluorescence immuno-chromatographic assay, photoelectric adjustment, light intensity, detection range.

## 1. Introduction

Fluorescence immunochromatographic assay (FICA) [1] is a popular quantitative detection technique that combines immunology, chromatography, and immunolabeling. FICA has the advantages of low cost, simple operation, fast detection speed, and high sensitivity, meeting various detection requirements. It is used for medical diagnosis, point of care testing, and laboratory work. The well-known applications include testings of food [2], [3], drugs [4], hormones [5], [6], virus [7], and environment [8], [9].

Much research so far has been conducted in developing high-performance FICA strip readers [10]–[13]. Based on operating principles and the hardware of the detection system, FICA strip readers can be classified into two categories: the imaging systems based on charge-coupled device (CCD) and the systems based on optical scanning. The CCD-based imaging system captures and analyzes test strip images with a CCD camera and a specific image processing algorithm. The main problem of the CCD-based imaging system is the high computational complexity of image processing. In literature, Yeh *et al.* [14] have presented an optical inspection system based on the Taguchi method, which can achieve better linearity and smaller standard deviation. Gao *et al.* [15] have developed a calibration strip for a FICA strip reader system that improves detection accuracy. For the scanning system, an optical module is developed to scan a test strip, and the obtained one-dimensional fluorescent signal is analyzed using a specific signal processing algorithm to obtain the test result. Gu *et al.* [13] have developed a portable fluorescence reader for C-reactive protein (CRP) detection with a good sensitivity of 0.1 mg/L. Yan *et al.* [16] have created a FICA-based biosensor for the rapid detection of *Yersinia pestis*.

For the FICA strip reader, it is critical to ensure that the concentration can be reliably and quantitatively measured in its working range. When integrated with different test strips, the same FICA strip reader can demonstrate different limits of detection (LoDs) and upper detection limits (UDLs), which determine the specific application range of the system. For instance, CRP concentration in serum can change due to the stimulation of various inflammations, and it can increase from less than 1  $\mu\text{g/mL}$  to 600–1000  $\mu\text{g/mL}$  at the peak of an acute-phase response [17]. In application to the Covid-19 viruses, the CRP indicator of concentration was found to be higher with the worsening of severity [18]. Therefore, it is necessary to ensure that the LoD and UDL of the system meet the detection requirements when the FICA strip reader is applied. Generally, the LoD can be improved by amplifying the associated signals. However, noise and interference will also be amplified, and useful signals may be amplified beyond the sampling range of the system, resulting in lower UDL [19]–[21]. Therefore, increasing the magnification alone cannot effectively extend the detection range of FICA strip readers.

In this paper, a photoelectric adjustment system was developed to overcome the above issue of the detection range in different applications. We first considered the impact of the detection parameters on the test results of the lateral flow immunoassay. We then proposed an adaptive system that can adjust the excitation light intensity and provide a stable background amplitude. The proposed system was applied to the FICA strip reader we have previously developed [15] to verify the effectiveness of our proposal. The ESEQuant Lateral Flow Reader (LFR) (developed by Qiagen, Germany) was used for benchmark comparisons.

## 2. The Photoelectric Adjustment Method

In this section, we will describe the proposed method with the FICA strip as the application structure.

### 2.1 Detection Mechanism of the FICA Strip

Generally, a FICA strip consists of a sample pad, an absorbent pad, a nitrocellulose membrane, a test line (T-line) and a control line (C-line) [22], [23]. The structure of the FICA strip is shown in Fig. 1(a). The T-line presents the concentration of the analyte, and the C-line confirms the validity

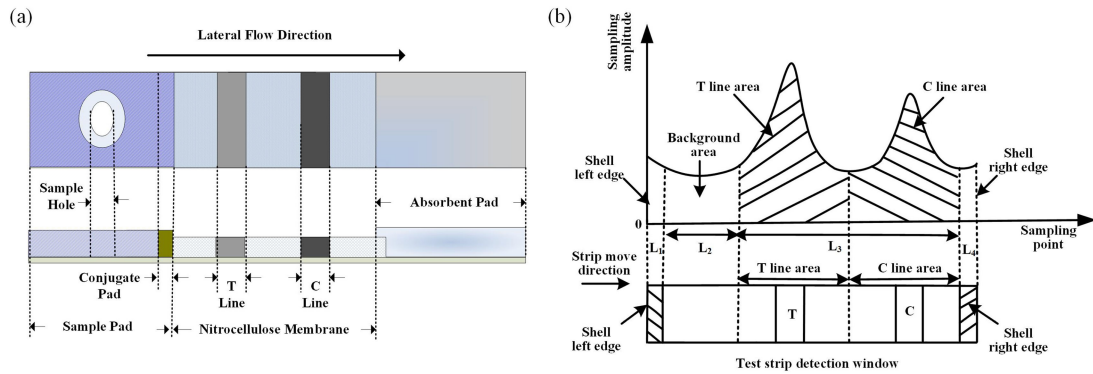


Fig. 1. (a) Structure of the FICA strip, (b) Fluorescence signal sample results compared with the test strip structure.

of the test. The fluorescent particles assemble in the T- and C-lines when a test is conducted. The concentration of the analyte is proportional to the emission light intensity of fluorescence particles, which are bonded to the antigen/antibody and both fixed on the NC membrane. The emission light is detected via the photoelectric sensor in the FICA strip reader. For a valid FICA strip, the sampling amplitude of the fluorescence signal usually has two peaks ( $L_3$ ) associated with the fluorescence intensity of the T-line and the C-line, and outside the two peaks is the background signal ( $L_2$ ), as shown in Fig. 1(b). Because the scan distance of the stepper motor is wider than the detection window,  $L_1$  and  $L_4$  are the left and right edges of the strip shell. Finally, fluorescence-intensity ratio of T-line to C-line ( $T/C$ ) is introduced to obtain the concentration of the analyte through the curve fitting.

During this detection process, how to choose a suitable baseline is critical. The shell edges  $L_1$  and  $L_2$  have the different reflection coefficients with the NC membrane. The background signal  $L_2$  is affected by the common-mode biochemical noise in the test strip and changes synchronously with  $L_3$ . Therefore,  $L_2$  is employed as the test baseline in this paper.

The two peaks area  $L_3$  with T- and C- lines, includes the main quantitative information for the test. Assume that  $I_0$  is the excitation light intensity,  $Y_F$  is the fluorescence efficiency,  $\varepsilon$  is the molar absorption coefficient,  $l$  is the optical path between the excitation light and the analyte, and  $c$  is the concentration of the fluorescence particles. Then the emission fluorescence intensity ( $I_f$ ) [24] is:

$$I_f = 2.3Y_F I_0 \varepsilon c l. \quad (1)$$

For the same test strip, the T-line and the C-line are irradiated by the same excitation light and labeled with the same fluorescent particles. Therefore,  $I_0$ ,  $Y_F$ ,  $\varepsilon$ , and  $l$  are equal in the T- and C-lines. Final, the eigenvalue ( $\lambda$ ) of the FICA strip is given by

$$\lambda = T/C = I_{fT}/I_{fC} = c_T/c_C, \quad (2)$$

where  $c_T$  and  $c_C$  are the fluorescent particle-concentrations of T- and C-lines, respectively.  $I_{fT}$  and  $I_{fC}$  are the fluorescence intensities of the T- and C-lines, respectively.

Based on (2), the test results depend only on the fluorescent particles concentrations in T- and C-lines. Therefore, when we use the ratio  $T/C$  as the eigenvalue, the test results are independent of the excitation light intensity variations.

## 2.2. Regulation of the Excitation Light Intensity

Fluorescent particles will transit from the ground state to the excited state under the irradiation of the excitation light. Given that the excited particles are unstable, they will release energy by emitting fluorescence and return to the original ground state. Since  $c$ ,  $Y_F$ ,  $l$  and  $\varepsilon$  are fixed values in (1),

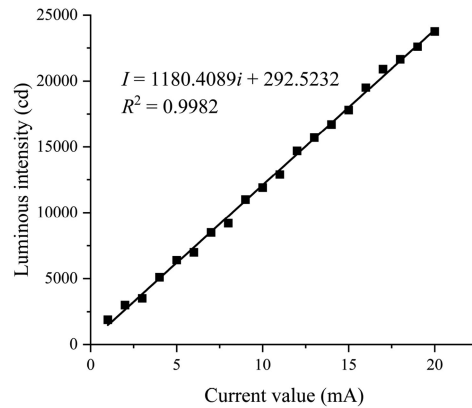


Fig. 2. Relationship between the current value of the light source and the luminous intensity.

the fluorescence intensity and the excitation light intensity are linearly related. So the stronger the excitation light is, the stronger the fluorescence intensity will be.

The silicon photodiode of Model S1122-14, is selected as the photoelectric converter of the FICA strip reader (for its short-circuit current is linearly related to the incident light intensity). The current generated by the photodiode is converted into a voltage signal by a trans-impedance amplifier. As a result, the fluorescence intensity  $I_f$  is linearly proportional to the voltage  $V_x$ . Thus,  $I_f$  of (1) is linearly related to  $V_x$ :

$$V_x = I_f = 2.3Y_F \varepsilon c l I_0. \quad (3)$$

The ultraviolet (UV) LED (T5H36) is used as the excitation light source. The relation between its current and luminous optical intensity generated can be obtained with a fiber optic spectrometer (USB4000-VIS-NIR, Ocean Optics). To obtain a better regulation effect, the characteristic curve is extracted with the current less than 20 mA. Fig. 2 shows the relationship between the current and intensity. With the goodness of fit ( $R^2$ ) reaches 0.9982, the relation can be expressed as

$$I_0 = \alpha i_x, \quad (4)$$

where  $I_0$  is the excitation light intensity,  $i_x$  is the input current of the LED, and  $\alpha$  is the proportional constant, respectively.

Substituting (4) into (3) reads

$$V_x = 2.3Y_F \varepsilon c l \alpha i_x = \beta i_x, \quad (5)$$

where  $\beta = 2.3Y_F \varepsilon c l \alpha$ . Since  $c$ ,  $l$ ,  $Y_F$ , and  $\varepsilon$  are fixed during the test,  $\beta$  is constant. In other words,  $V_x$  and  $i_x$  are linearly related. Therefore, by changing  $i_x$  in the range of 0-20 mA,  $V_x$  can be adjusted to the appropriate sampling range of the system to achieve the purpose of range adjustment.

### 2.3 Optical Module

A high-precision optical module is much desired to improve the accuracy of the FICA strip readers. The module we develop uses a UV LED, a few lenses, and a filter, as shown in Fig. 3. It has two convex lenses (A and B), one cylindrical lens, and one dichroic lens. Lens A is used to collimate the UV light, which is further reflected by the dichroic lens and then enters the test strip through the cylindrical lens. The dichroic lens is placed at an angle to reflect the UV light vertically to the cylindrical lens, which shapes the UV light into a linear beam for better excitation. Given that the shapes of the T- and C-lines of the test strip are rectangular, the incident light should be a rectangular spot to make the best use of the fluorescent signals. The LED is on the left side

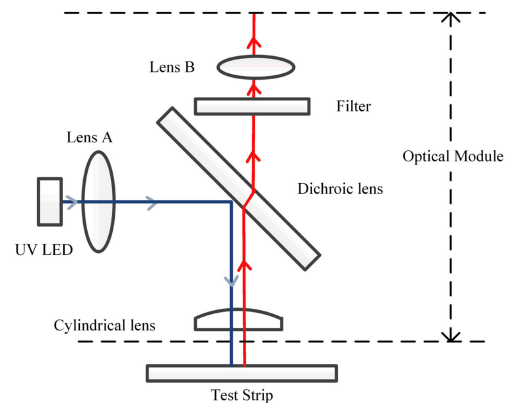


Fig. 3. Schematic diagram of the optical module.

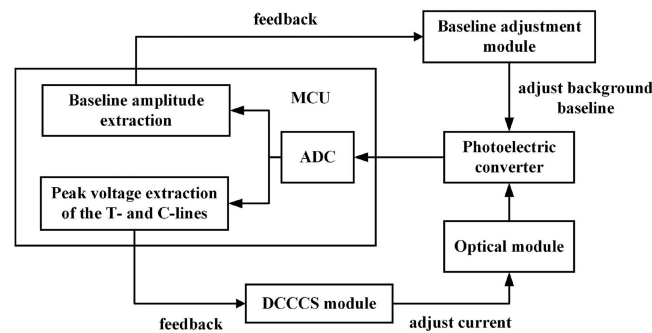


Fig. 4. Diagram of the proposed photoelectric adjustment system for the FICA strip reader.

of the convex lens and can be adjusted for its angle. Moreover, the size of the light spot should be the same as the size of the inspection window.

### 3. The Proposed Photoelectric Adjustment System with Range Extended

With the FICA strip and the optical module described in the previous section, we propose a photoelectric adjustment system to adjust the detection range of the FICA strip reader.

#### 3.1 The Photoelectric Adjustment System

The photoelectric adjustment system is shown in Fig. 4. The FICA strip reader can detect the electrical signal of the test strip through the analog-to-digital converter (ADC). Then the micro-controller unit (MCU) extracts the baseline amplitude and the peak voltages of the T- and C-lines. The range adjustment of the FICA strip reader is achieved by the feedback adjustment of the digitally controlled constant-current source (DCCCS) module and baseline adjustment module.

The proposed system of Fig. 4 is a negative feedback system that can adapt to the changes of low- and high-concentration strip for better performances. In the case of a low-concentration test strip, the fluorescence is weak, resulting in a low signal-to-noise ratio (making the MCU difficult to separate the baseline signal and the peak line signal). The proposed system will then increase the LED input current to enhance the excitation light intensity. Accordingly, the emission fluorescence intensity is increased to avoid the useful signal being drowned by noise. In the case of a high-concentration test strip, the emission fluorescence intensity may exceed the sampling amplitude range of the ADC. Then the proposed system will decrease the input current of the



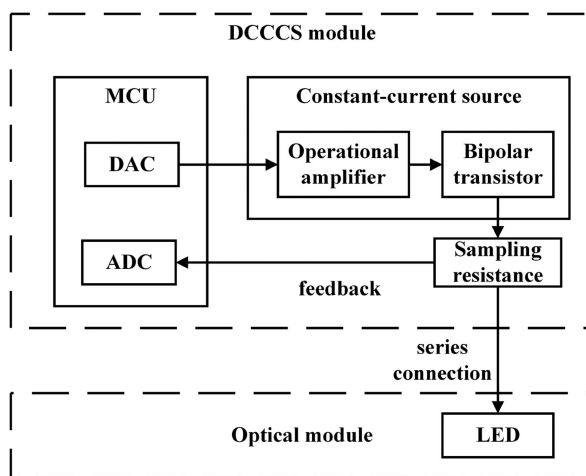


Fig. 5. Diagram of the DCCCS module.

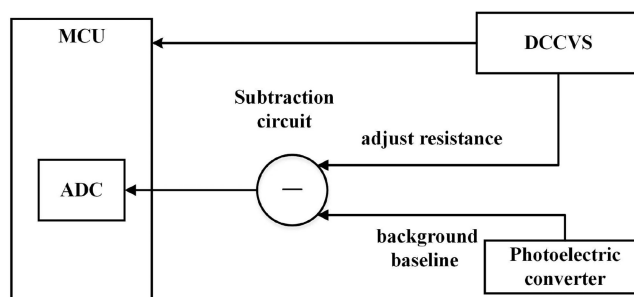


Fig. 6. Diagram of the baseline adjustment module.

LED to weaken the excitation light intensity. Accordingly, the emission fluorescence intensity is decreased to the sampling range of the system. In other words, the proposed photoelectric adjustment system will automatically adjust and obtain the electrical signals within the optimal detection range of the proposed FICA strip reader.

The key component of the proposed photoelectric adjustment system is the DCCCS module, which supplies an adjustable current to the LED in the optical module. As shown in Fig. 5, the MCU provides an adjustable current to the LED by adjusting the output of the digital-to-analog converter (DAC). In addition, a feedback mechanism is used to ensure the stability of the supplied current. When the current flowing through the LED changes, the voltage over the sampling resistor connected in series with the LED changes accordingly and is fed back to the MCU through the ADC. The MCU compares the preset value with the sampling value and uses the compared result to control the DAC to output the proper voltage for current compensation.

During the immune-reaction on the FICA test strip, a small portion of fluorescent particles will remain in the background area due to the rate variation of particle movement and the self-fluorescence of the sample matrix. Therefore, the baseline of the background signal will increase as the excitation light intensity increases. It leads to the baseline signal unstable during each test and increases the result discreteness. In order to overcome this problem, a baseline adjustment module is developed, as shown in Fig. 6. The module consists of a digital controlled constant-voltage source (DCCVS) and a subtraction circuit. When the uncertain background baseline signal is detected by the optical module and photoelectric converter, the MCU adjusts the dropout voltage of DCCVS by adjusting the output resistance of the digital potentiometer. Therefore, the output of the subtraction

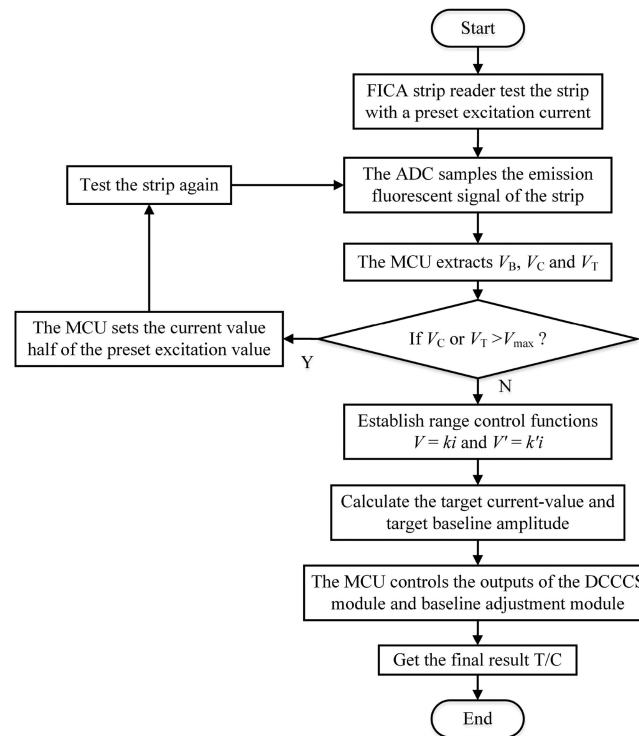


Fig. 7. Range adjustment process of the photoelectric adjustment system.

circuit is kept constant. The constant is as small as possible to ensure an adequate range of the strip reader. As a result, the sampling voltage of the background baseline will be stable even when the excitation light intensity varies with different strips.

### 3.2 Adjustment of the Detection Range

The range adjustment process of the photoelectric adjustment system is shown in Fig. 7. It involves five steps. Firstly, the FICA strip reader is used to test the strip with a preset excitation current value. Secondly, the ADC samples the emission fluorescent signal of the strip. Thirdly, the MCU extracts the baseline amplitude ( $V_B$ ), the peak voltage of the T-line ( $V_T$ ) and the peak voltage of the C-line ( $V_C$ ). If  $V_T$  or  $V_C$  exceeds the maximum sampling amplitude of ADC (assumed to be  $V_{max}$ ), the MCU controls the DCCCS module to output half of the preset excitation current value to the LED and then retest the strip. Fourthly, the range control functions are established to calculate the target current-value and the target baseline amplitude. Finally, the MCU controls the output of the DCCCS module and baseline adjustment module according to the calculated target current value and target background amplitude to realize the adjustment of the detection range.

According to (5), when the concentration of the strip is fixed, the current value of the light source is linearly related to the peak voltage in the electrical signal curve. Assuming that  $i$  is the current value of the light source and  $V$  is the peak voltage in the electrical signal curve, it is obvious that they satisfy the mathematical model of  $V = ki$ . The proportional coefficient  $k$  is calculated through the preset excitation current value and the obtained peak voltage. The target current-value is the ratio of the maximum sampling amplitude of the ADC ( $V_{max}$ ) to the proportional coefficient  $k$ . The MCU compares the target current-value with the allowable maximum current value (20mA). Then, it controls the DCCCS module to output a specified current to the LED.

Similarly, when  $V'$  is assumed to be the baseline amplitude, the current value of the light source and the baseline amplitude also satisfy the mathematical model of  $V' = k'i$ . The proportional



TABLE 1  
Test Results Under Different Current Values

Current value (mA)	7.81 ( $\mu\text{g/mL}$ )	31.25 ( $\mu\text{g/mL}$ )	125 ( $\mu\text{g/mL}$ )
1	0.2411	0.9307	2.8910
2	0.2431	0.9273	2.9167
5	0.2467	0.9159	2.8983
10	0.2476	0.9267	2.9091
15	0.2474	0.9309	2.9004
20	0.2480	0.9290	2.8985
Average Value	0.2457	0.9268	2.9023
Standard Deviation	0.0029	0.0056	0.0091
Relative Standard Deviation	1.16%	0.60%	0.31%

coefficient  $k'$  is calculated through the preset excitation current value and the obtained baseline amplitude. The target baseline amplitude is  $k'$  times of the target current value. The MCU adjusts the resistance of the digital potentiometer to keep the subtraction circuit output as a constant. Thus, the baseline adjustment module can provide a stable baseline amplitude to ensure the detection repeatability, as well as expand the available scope of the ADC.

## 4. Experiment and Results

We performed experiments to verify the effectiveness of our proposed method and system. In the experiments, we compared the performance of the FICA strip reader with and without the photoelectric adjustment. Also, we selected the ESEQuant LFR for the comparison purpose. All experiments were carried out by dropping CRP standard solution into CRP test strips (Triplex International Biosciences Co., LTD., Xiamen, China).

### 4.1 Impact of the Current Value on Detecting Results

According to (2), the test results only depend on the concentration of the fluorescent particles in the T- and C-lines. Moreover, the results have no relation to the excitation light intensity. To study the impact of the variations of the current value of the light source on the testing results ( $T/C$ ), three different concentrations of CRP solution were used for testing. The test results under different current values of the light source are shown in Table 1.

Fig. 8 shows that as the current value of the light source increases, the test results ( $T/C$ ) are basically unchanged. In addition, the relative standard deviation of all three experiments were less than 1.16%, indicating that changing the current value of the light source had essentially no impact on the test results as expected theoretically.

### 4.2 Background Baseline Adjustment

To assess the performance of the baseline adjustment module, five test strips with different CRP concentrations were selected for background baseline detection. Table 2 presents the results.

As shown in Table 2, the background baseline drifted greatly before adjustment. To reduce the effect of background baseline drift, the MCU set the background baseline at a constant voltage, 100 mV, by controlling the resistance of the digital potentiometer. After adjustment, the baseline amplitude was stable near 100 mV with a maximum relative error less than 4%. Therefore, the baseline adjustment module could satisfy the requirements of baseline amplitude control.

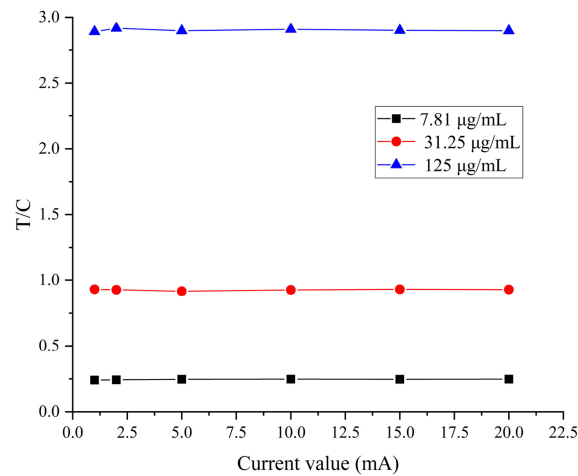


Fig. 8. Relationship between the current value of the light source and the test result.

TABLE 2  
Comparison of Baseline Amplitude Before and After Adjustment

Strip	Before Adjustment (mV)	After Adjustment (mV)	Differences to 100mV (mV)
1	1139	104	4
2	1376	102	2
3	1272	99	1
4	1302	103	3
5	1183	99	1

TABLE 3  
Repeatability Test of the FICA Strip Reader

Test Times	7.81 (µg/mL)	31.25 (µg/mL)	125 (µg/mL)
1	0.2469	0.9269	2.8981
2	0.2458	0.9306	2.9020
3	0.2439	0.9284	2.8953
Average Value	0.2455	0.9286	2.8985
Standard Deviation	0.2455	0.9286	2.8985
Relative Standard Deviation	0.62%	0.20%	0.12%

#### 4.3 Range Extension

To verify the repeatability of the FICA strip reader, three repeated tests were performed on CRP solution of different concentrations. The test results are shown in Table 3. It can be found that in the repeatability experiment, the FICA strip reader shows good repeatability with the relative standard deviation less than 0.62%.

To verify the accuracy of the FICA reader and the effect of range adjustment, a series of CRP solution were detected with the FICA strip reader and then with the ESEQuant LFR. As shown in Table 4, the detection range of the FICA strip reader was 1.95–256 µg/mL before adjustment.

TABLE 4

Comparison of Detection Ranges Between the FICA Strip Reader and the ESEQuant LFR

Concentration ( $\mu\text{g/mL}$ )	$T/C$ Before Adjustment	$T/C$ After Adjustment	ESEQuant LFR $T/C$
2048	—	—	—
1024	—	22.7272	—
512	—	12.0479	—
256	6.3066	6.3275	—
125	2.8551	2.8985	—
31.25	0.9493	0.9286	0.8491
7.81	0.2565	0.2455	0.2425
1.95	0.04859	0.04773	0.0490
1	—	0.02216	0.0281
0.5	—	—	—

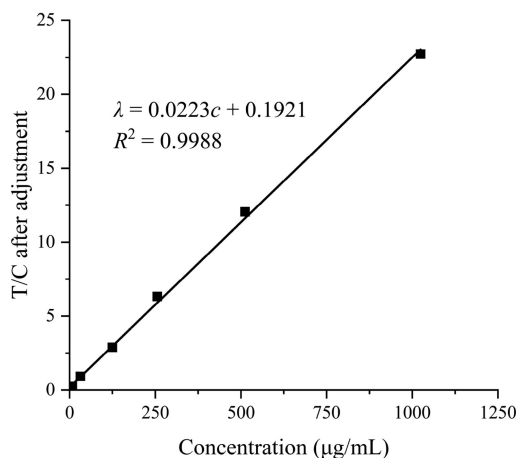


Fig. 9. Linearity of test results after using the photoelectric adjustment method.

After adjustment, the detection range was extended to 1–1024  $\mu\text{g/mL}$ . Furthermore, the UDL of the FICA strip reader is much higher than that of the ESEQuant LFR. Therefore, the photoelectric adjustment method can effectively extend the detection range of the FICA strip reader.

#### 4.4 Linearity Test

The fitted curve was obtained by fitting the concentration of the test strip and the  $T/C$  after adjustment. It is shown in Fig. 9.

The linear relationship obtained by using the least square method is

$$\lambda = 0.0223c + 0.1921, \quad (6)$$

where  $\lambda$  is the  $T/C$  after adjustment, and  $c$  is the concentration of the test strip. The goodness of fit ( $R^2$ ) reaches 0.9988, indicating a good linear relationship between the test results and the concentration of the test strip within the measurable range.

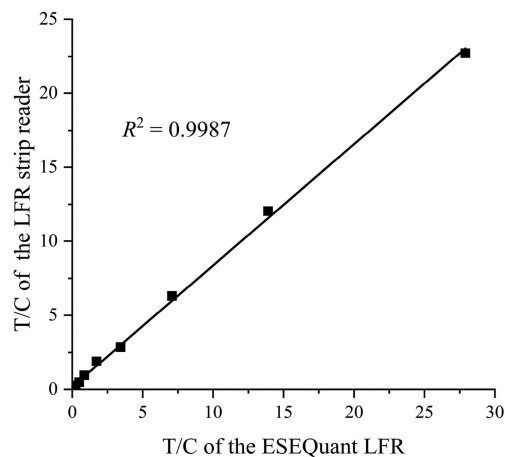


Fig. 10. Correlation of test results between the FICA strip reader and the ESEQuant LFR.

#### 4.5 Accuracy Test

The accuracy test was performed by analyzing the correlation of the test results between the FICA strip reader and the ESEQuant LFR. The results are shown Fig. 10. As seen, the detection range of the ESEQuant LFR was linearly extended to that of the FICA strip reader.

The goodness of fit ( $R^2$ ) reaches 0.9987, indicating a good correlation between the test results of the FICA strip reader and the ESEQuant LFR. Therefore, the FICA strip reader after adjustment could perform accurate tests.

### 5. Conclusion

In this work, we study the relationship between the excitation intensity and fluorescence intensity and present a photoelectric range-adjustment method. Based on the proposed method, we propose a photoelectric adjustment system to expand the detection range of the FICA strip reader. It consists of a DCCCS module and a baseline adjustment module. The DCCCS module adjusts the excitation light intensity by changing the LED current so that the final measured electrical signal curve can be within the optimal detection range. The baseline adjustment module keeps the output of the system constant, which not only solves the problem of background baseline drift but also expands the available range of ADC. The experiments verify that variations of the current of the light source had little effect on the test results, proving the correctness of the photoelectric adjustment method.

The proposed system was incorporated into the FICA strip reader we had previously developed. The test results showed that the stability of the background baseline is significantly improved, and the detection range of the FICA strip reader is extended from 1.95–256  $\mu\text{g/mL}$  to 1–1024  $\mu\text{g/mL}$  after the photoelectric adjustment method is applied. Moreover, the goodness of fit ( $R^2$ ) reaches 0.9987 in the accuracy test, indicating that the accuracy of the FICA strip reader is in good agreement with the ESEQuant LFR. Therefore, the photoelectric adjustment method is shown to extend the detection range of the FICA strip reader effectively. In addition, it is worth to mention that the photoelectric adjustment method is not only suitable for FICA strip readers, but also for other strip readers based on optical scanning. They usually perform analyte detection under fixed detection parameters, so their detection range is fixed. The proposed method provides a new idea for the range adjustment of the strip reader based on optical scanning. First of all, the designed system should be able to provide the adjustment of detection parameters. Then, the variable range of the detection parameters of the system should be determined by considering its relation with the

test results. Finally, it is necessary to adjust the measured signal within the variable range of the detection parameters to realize the range expansion of the system.

## References

- [1] T. K. Kim, S. W. Oh, S. C. Hong, Y. J. Mok, and E. Y. Choi, "Point-of-care fluorescence immunoassay for cardiac panel biomarkers," *J. Clin. Lab. Anal.*, vol. 28, no. 6, pp. 419–427, Nov. 2014.
- [2] M. J. Raeisossadati *et al.*, "Lateral flow based immunobiosensors for detection of food contaminants," *Biosensors Bioelectron.*, vol. 86, pp. 235–246, Dec. 2016.
- [3] G. Tan, Y. Zhao, M. Wang, X. Chen, B. Wang, and Q. X. Li, "Ultrasensitive quantitation of imidacloprid in vegetables by colloidal gold and time-resolved fluorescent nanobead traced lateral flow immunoassays," *Food Chem.*, vol. 311, no. 7, May 2020, Art. no. 126055.
- [4] M. Wang, L. Q. Guo, M. Yu, and H. Zhao, "The application of a lateral flow immunographic assay to rapidly test for dexamethasone in commercial facial masks," *Anal. Bioanalytical Chem.*, vol. 411, no. 22, pp. 5703–5710, Sept. 2019.
- [5] A. Chamorro-Garcia, A. de la Escosura-Muniz, M. Espinoza-Castaneda, C. J. Rodriguez-Hernandez, C. de Torres, and A. Merkoci, "Detection of parathyroid hormone-like hormone in cancer cell cultures by gold nanoparticle-based lateral flow immunoassays," *Nanomedicine-Nanotechnol. Biol. Med.*, vol. 12, no. 1, pp. 53–61, Jan. 2016.
- [6] S. Choi, J. Hwang, S. Lee, D. W. Lim, H. Joo, and J. Choo, "Quantitative analysis of thyroid-stimulating hormone (TSH) using SERS-based lateral flow immunoassay," *Sensors Actuators B-Chem.*, vol. 240, pp. 358–364, Mar. 2017.
- [7] F. Wu *et al.*, "Multiplexed detection of influenza A virus subtype H5 and H9 via quantum dot-based immunoassay," *Biosensors Bioelectron.*, vol. 77, pp. 464–470, Mar. 2016.
- [8] L. H. Liu, X. H. Zhou, J. S. Wilkinson, P. Hua, B. D. Song, and H. C. Shi, "Integrated optical waveguide-based fluorescent immunosensor for fast and sensitive detection of microcystin-LR in lakes: Optimization and analysis," *Sci. Rep.*, vol. 7, no. 9, Jun. 2017, Art. no. 3655.
- [9] A. Sanchis, J. P. Salvador, and M. P. Marco, "Multiplexed immunochemical techniques for the detection of pollutants in aquatic environments," *Trac-Trends Anal. Chem.*, vol. 106, pp. 1–10, Sept. 2018.
- [10] V. Venkatraman and A. J. Steckl, "Integrated OLED as excitation light source in fluorescent lateral flow immunoassays," *Biosensors Bioelectron.*, vol. 74, pp. 150–155, Dec. 2015.
- [11] K. B. Chowdhury, J. Joseph, J. K. Vasani, and M. Sivaprakasam, "ImQuant - An image based fluorescence reader for quantitative lateral flow immunoassays," In *Proc. 38th Annu. Int. Conf. IEEE Eng. Med. Biol. Soc.*, pp. 5152–5155, New York, NY, USA: IEEE, Aug. 2016.
- [12] Z. J. Chen *et al.*, "Development of a low-cost, simple, fast and quantitative lateral-flow immunochromatographic assay (ICA) strip for melatonin in health foods," *Food Agricultural Immunol.*, vol. 30, no. 1, pp. 497–509, Jan. 2019.
- [13] Y. B. Gu, Y. L. Yang, J. Zhang, S. X. Ge, Z. H. Tang, and X. B. Qiu, "Point-of-care test for C-reactive protein by a fluorescence-based lateral flow immunoassay," *Instrum. Sci. Technol.*, vol. 42, no. 6, pp. 635–645, Nov. 2014.
- [14] C. H. Yeh, Z. Q. Zhao, P. L. Shen, and Y. C. Lin, "Optimization of an optical inspection system based on the Taguchi method for quantitative analysis of point-of-care testing," *Sensors*, vol. 14, no. 9, pp. 16148–16158, Sept. 2014.
- [15] Y. M. Gao, J. C. Wei, P. U. Mak, M. I. Vai, M. Du, and S. H. Pun, "Development of a calibration strip for immunochromatographic assay detection systems," *Sensors*, vol. 16, no. 7, Jul. 2016, Art. no. 1007.
- [16] Z. Q. Yan *et al.*, "Rapid quantitative detection of yersinia pestis by lateral-flow immunoassay and up-converting phosphor technology-based biosensor," *Sensors Actuators B-Chem.*, vol. 119, no. 2, pp. 656–663, Dec. 2006.
- [17] K. O. Pietila, A. P. Harmoinen, J. Jokiniitty, and A. I. Pasternack, "Serum C-reactive protein concentration in acute myocardial infarction and its relationship to mortality during 24 months of follow-up in patients under thrombolytic treatment," *Eur. Heart J.*, vol. 17, no. 9, pp. 1345–1349, Sept. 1996.
- [18] F. Shi *et al.*, "Association of viral load with serum biomarkers among COVID-19 cases," *Virology*, vol. 546, pp. 122–126, Jul. 2020.
- [19] S. Z. Lv, K. Y. Zhang, L. Zhu, and D. P. Tang, "ZIF-8-Assisted NaYF<sub>4</sub>:Yb,Tm@ZnO converter with exonuclease III-powered DNA walker for near-infrared light responsive biosensor," *Anal. Chem.*, vol. 92, no. 1, pp. 1470–1476, Jan. 2020.
- [20] L. T. Huang, J. L. Chen, Z. H. Yu, and D. P. Tang, "Self-powered temperature sensor with seebeck effect transduction for photothermal-thermoelectric coupled immunoassay," *Anal. Chem.*, vol. 92, no. 3, pp. 2809–2814, Feb. 2020.
- [21] Z. Z. Yu, G. N. Cai, X. L. Liu, and D. P. Tang, "Pressure-based biosensor integrated with a flexible pressure sensor and an electrochromic device for visual detection," *Anal. Chem.*, vol. 93, no. 5, pp. 2916–2925, Feb. 2021.
- [22] K. Y. Zhang, J. C. Wu, Y. N. Li, Y. R. Wu, T. F. Huang, and D. P. Tang, "Hollow nanogold microsphere-signalized lateral flow immunodipstick for the sensitive determination of the neurotoxin brevetoxin B," *Microchimica Acta*, vol. 181, nos. 11–12, pp. 1447–1454, Aug. 2014.
- [23] Z. Q. Gao *et al.*, "Platinum-Decorated gold nanoparticles with dual functionalities for ultrasensitive colorimetric in vitro diagnostics," *Nano Lett.*, vol. 17, no. 9, pp. 5572–5579, Sep. 2017.
- [24] T. Frost, "Quantitative analysis," in *Encyclopedia of Spectroscopy and Spectrometry*, 3rd ed., J. C. Lindon, G. E. Tranter, and D. W. Koppenaal, Eds., Amsterdam, NH, Holland: Elsevier Science, 2017, pp. 811–815.